

Retrieval of the vertical rainfall structure from the MADRAS imager data of the Megha-Tropiques satellite

C. Balaji^{1,*} and K. Srinivasa Ramanujam²

¹Department of Mechanical Engineering, Indian Institute of Technology Madras, Chennai 600 036, India

²Department of Electrical and Computer Engineering, Colorado State University, Fort Collins 80523, USA

A physically based algorithm for the retrieval of vertical cloud and rain structure from the MADRAS imager data of Megha-Tropiques is developed. A community-developed meso-scale numerical weather simulation software, WRF, has been used for simulation of thermodynamic, cloud and rain profiles for a cyclone case. The WRF simulated profiles in conjunction with two of the rain-measuring instruments on-board the TRMM satellite, the TMI and the TRMM PR, are used as a priori cloud and rain profiles database. These profiles were input to an in-house radiative transfer code. Brightness temperatures at MADRAS imager frequencies were simulated to complete the generation of a priori database. Brightness temperatures were also simulated for TMI channels for comparison, wherever possible.

Sample MADRAS data were downloaded and retrievals were performed for the MADRAS channels. The retrieved wind speed, column-integrated liquid water and surface rain rate were compared against the Level 2 data of Megha-Tropiques mission. A comparison of daily averaged rain rate with TMI retrievals was also made. The results show that the retrieval algorithm is robust and able to retrieve the vertical cloud and rain structure even in the absence of a radar on-board the Megha-Tropiques.

Keywords: Geophysical retrievals, inverse problems, Megha-Tropiques, passive microwave remote sensing.

MEGHA-TROPIQUES¹ is a joint space mission between the Indian Space Research Organization (ISRO), India and the Centre National d'Études Spatiales (CNES), France. The satellite was launched successfully through ISRO's Polar Satellite Launch Vehicle (PSLV-C18) on 12 October 2011. The primary goal of Megha-Tropiques is to retrieve geophysical parameters from simultaneous observations of precipitation from a suite of instruments on-board; a microwave radiometer named Microwave Analysis and Detection of Rain and Atmospheric Systems (MADRAS), visible and infrared scanner named Scanner for Radiation Budget (ScaRaB) and a microwave sounder

named *Sondeur Atmospherique du Profil d'Humidite Intertropicale par Radiometrie (SAPHIR)*.

The present study focuses on developing a Bayesian-based algorithm to retrieve the vertical profiles of pressure, temperature and humidity, collectively known as thermodynamic profiles, and cloud water, cloud ice, rain and precipitating ice (includes snow, graupel, hail, etc.), collectively known as hydrometeor profiles, up to a height of 18 km from the Earth's ocean surface from MADRAS brightness temperatures.

The primary rain-measuring instrument, MADRAS, has frequencies similar to the Tropical Rainfall Measuring Mission² (TRMM)'s Microwave Imager (TMI), with an additional 157 GHz instead of the low frequency 10 GHz channels. The channel frequencies of MADRAS and their characteristics are shown in Table 1 (reproduced from Megha-Tropiques satellite sensor characteristics report, ISRO, July 2006).

MADRAS is a conical scanning radiometer with a satellite viewing angle of 56° with respect to the Earth's surface and a horizontal resolution of 6 km at 157 GHz. The combination of low frequency (18.7, 23.8 and 36.5 GHz) and high frequency (89 and 157 GHz) channels provides a valuable insight in observing light, medium, high rain and ice concentration from a precipitating system. A relationship between various rain parameters and brightness temperatures can be established through the radiative transfer equation that governs the physics of the emitting, absorbing and scattering rainy atmosphere.

It has been observed by various investigators³⁻⁵ that the presence of hydrometeors suspended in air tends to polarize the radiative transfer energy emitted by the Earth's surface when passing through them. Hence, in addition to considering the polarization of emitted signal from the ocean surface, radiative transfer should also consider polarization from suspended and precipitating particles.

For the present study, an in-house developed polarized radiative transfer equation (PRTE) written in FORTRAN⁶ was used to simulate the brightness temperatures at MADRAS frequencies for various rain conditions. The initial thermodynamic and hydrometeor profiles for a layered plane parallel atmosphere as shown in Figure 1 were taken from the numerical simulation of several precipitating

*For correspondence. (e-mail: balaji@iitm.ac.in)

Table 1. Channels of MADRAS and their main characteristics

Frequency (GHz)	Polarization	Pixel size (km)	Main characteristics
18.7	<i>H, V</i>	≤ 40	Rain above oceans
23.8	<i>V</i>	≤ 40	Integrated water vapour
36.5	<i>H, V</i>	≤ 40	Liquid water in clouds, rain above sea
89	<i>H, V</i>	≤ 10	Convective rain areas over land and sea
157	<i>H, V</i>	≤ 6	Ice at cloud tops

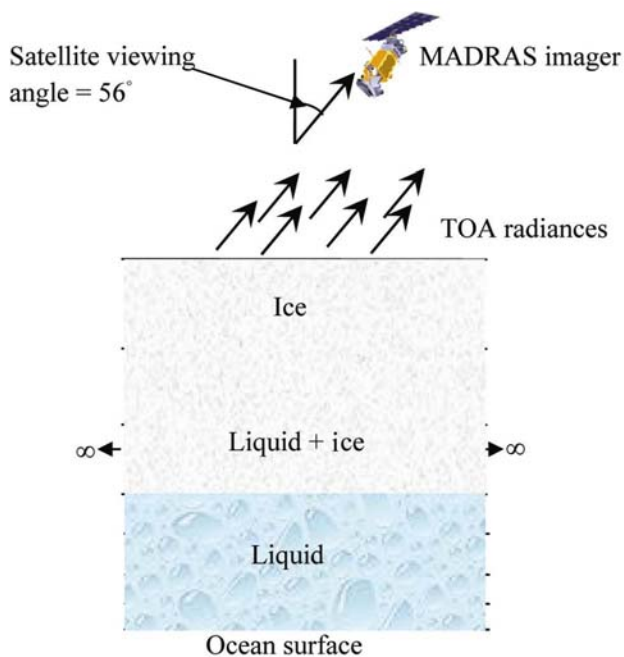


Figure 1. Schematic of a layered raining atmosphere.

systems using a community meso-scale numerical weather prediction model, Weather Research and Forecast (WRF).

As the first step towards solving the PRTE code, the atmospheric profiles are converted into radiation interaction parameters such as single scattering albedo, extinction coefficient and phase matrix. An appropriate drop size distribution (DSD) model is assumed for calculating interaction parameters for cloud and precipitating profiles. For suspended particles, modified gamma distribution is used. The modified gamma distribution with four parameters is given by

$$n(r) = ar^\alpha \exp(-br^\gamma). \tag{1}$$

Here r denotes the radius of a rain drop. The modified gamma expression is related to the mass density (for liquid or solid) by the following expression

$$m = \int_0^\infty \left(\frac{4}{3}\pi r^3\right) \rho n(r) dr$$

$$= a\rho \left(\frac{4\pi}{3\gamma}\right) \left(\frac{\alpha}{\gamma}\right)^{-(\alpha+4)/\gamma} r_c^{\alpha+4} \Gamma\left(\frac{\alpha+4}{\gamma}\right), \tag{2}$$

where Γ and ρ represent the gamma distribution function and concentration of each of the hydrometeors (precipitating water, precipitating ice, cloud liquid water, cloud ice) respectively. The critical radius of a rain drop, r_c appearing in eq. (2) is given by

$$r_c = (\alpha/\gamma\beta)^{1/\gamma}. \tag{3}$$

A special case of the modified gamma distribution can be obtained by letting $\alpha = 0$, $\gamma = 1$ and $b = f(R_r)$, where R_r denotes rain rate in mm/h.

$$n(r) = a \exp(-f(R_r)r). \tag{4}$$

when $a = 16 \times 10^6$, $f(R_r) = 8200R_r^{-0.21}$, eq. (4) becomes the well-known Marshall Palmer distribution⁷. This distribution is used in the present study as the DSD model for precipitating water and ice parameters.

The constants appearing in eqs (2) and (3) are adjusted such that the radiation interaction parameters match the observations at different frequencies and temperatures⁸.

Polarized radiative transfer equation

The radiative transfer energy emerging from the Earth's ocean surface, passing through a raining atmosphere, can be modelled in the form of the radiative transfer equation⁹ given by

$$\mu \frac{dI}{d\tau}(\tau, \mu, \phi) = -I(\tau, \mu, \phi)$$

$$+ \frac{\tilde{\omega}}{4\pi} \int_0^1 \int_{-1}^1 P(\mu, \phi; \tilde{\mu}, \tilde{\phi}) d\tilde{\mu} d\tilde{\phi} + (1 - \tilde{\omega}) B(T) \begin{bmatrix} 1 \\ 0 \\ 0 \\ 0 \end{bmatrix}, \tag{5}$$

where μ, ϕ denote the two angles in the spherical coordinate system, $\tilde{\omega}$ represents the single scattering albedo, τ denotes the optical thickness of the atmosphere, I denotes the polarized radiative transfer field in the form of Stokes vectors (I, Q, U, V), P denotes the scattering phase function and B denotes Planck's blackbody function. According to eq. (5), the net intensity emerging out from the top of the atmosphere (TOA) in the direction θ is determined by the combined effect of absorption and out-scattering

(extinction), emission and in-scattering (augmentation) due to the presence of participating particles in the atmosphere.

The sea surface characterized by its temperature, salinity, wind speed, pressure and humidity acts as the bottom boundary surface, and the TOA exposed to space at 4 K is considered as the top surface boundary condition to solve eq. (5).

The coordinate system is defined such that τ increases downwards and μ is positive in the lower hemisphere. The radiation is axisymmetric in the azimuth direction and is represented in terms of a Fourier series. The discretization in the zenith angle is done using Gaussian quadrature points. The radiance field is represented by the Stokes parameters, quadrature zenith angles and Fourier azimuth modes.

Solution to PRTE is obtained by solving eq. (5) subject to the boundary conditions using the adding and doubling method. In the adding and doubling method, the interaction parameters are calculated for a homogenous sub-layer and are doubled till the desired layer thickness is reached and then added to the next layer of different thickness.

Generation of database

Cyclonic events that originated in the north Indian Ocean region bounded between 60E and 110E, 0N and 25N during 2003–2010 have been considered for the generation of the database. Fourteen cyclone events have been observed during this period, all of which had made their landfall along the coastal regions of India, Myanmar and Bangladesh. The initial and boundary conditions of these 14 cyclones are obtained from the National Center for Environmental Protection's (NCEP's) final analysis (FNL) data. The FNL data are updated every 6 h and are available in 1° grid resolution and at 26 vertical levels from 1000 to 10 hPa. The run time for the WRF model was chosen such that the model was able to capture the features of the cyclone at various stages of evolution (initial, mature and landfall stages).

The governing equations are cast in flux form and solved using the Advanced Research WRF (ARW) dynamic solver^{10–12}. The dynamic solver integrates the compressible, non-hydrostatic Euler equations and solves the governing equations using the Runge Kutta third-order scheme. The model integration time was 15 sec. WSM3 simple ice scheme was used to model the microphysics of the rain event, while Grell–Devenyi ensemble was used for cumulus parameterization. The WSM3 scheme considers microphysical processes of ice above the 0° isotherm. However, the scheme does not consider melting of snow or super-cooled water.

The outputs from the WRF model simulations include pressure, temperature, humidity, rain, snow and cloud water/ice mixing ratios. The mixing ratios are converted

to volume density before the profiles are input to the PRTE code.

Results and discussion

The WRF-simulated thermodynamic and hydrometeor profiles together with sustainable wind speed, sea surface temperature, sea surface pressure and sea level humidity are provided as input to the PRTE code. A constant salinity of 35 ppm has been assumed for the ocean surface. The WRF-generated hydrometeor profiles are converted to radiation interaction parameters with an assumed DSD, as explained in the previous section.

Simulations for the 157 GHz brightness temperature

It has been observed previously in the literature that the high-frequency channels are more sensitive to rain from ice clouds due to the effect of scattering. A study was conducted in order to ascertain the performance of this channel. The PRTE code was executed to simulate brightness temperature (BT) of a tropical cyclone MALA for the 157 GHz channel of the MADRAS imager. On 25 April 2006 the tropical cyclone 02B intensified further and evolved into a cyclone named MALA.

The WRF model simulated thermodynamic and hydrometeor profiles using NCEP FNL data for cyclone MALA were used as input to the PRTE code. The PRTE code simulated BTs at MADRAS frequencies. Figure 2 shows the BTs corresponding to the 157 GHz channel for the vertical and horizontal polarizations. TMI-measured BTs at 85 GHz *V*, *H* channels for the rain scene under consideration are shown in Figure 3 for comparison. A difference of about 50 K near heavily precipitating areas of the storm has been observed between the 157 GHz channel simulations and the 85 GHz channel observations. This difference reduces for low and medium rain areas of the storm. This observation suggests that BTs corresponding to the 157 GHz channel from the MADRAS imager can play an important role in retrieval of precipitating ice and heavy rain.

Generation of a priori database for retrievals

The thermodynamic and hydrometeor profiles simulated by WRF are subjected to model errors such as the assumption of the same set of physics options for all pixels irrespective of the scale effects and variation in rainfall rates in larger areas. In order to account for these errors, the WRF-generated profiles are matched up with two of the rain-measuring instruments on-board the TRMM satellite¹³. In the first step, the rain profiles are matched up with TRMM's Precipitation Radar (PR)-observed rain rate using a non-commercial radar simulation package, Quickbeam as the forward model.

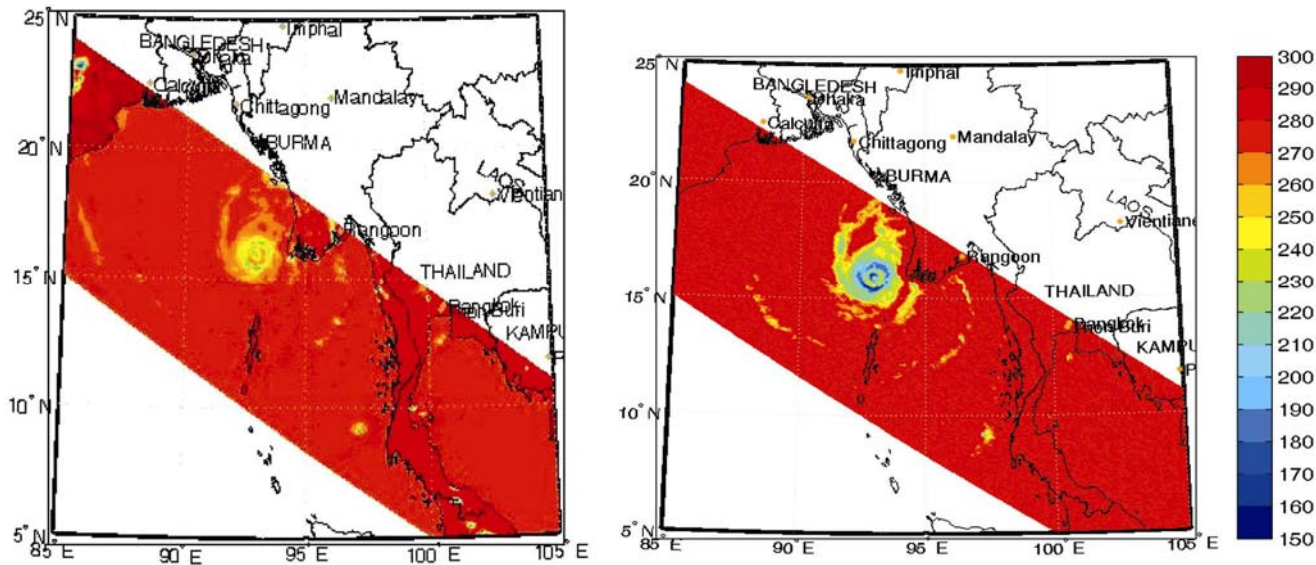


Figure 2. Simulation of 157 GHz brightness temperature (K) for tropical cyclone MALA in vertical (left) and horizontal (right) polarization (geographical boundaries are not to scale).

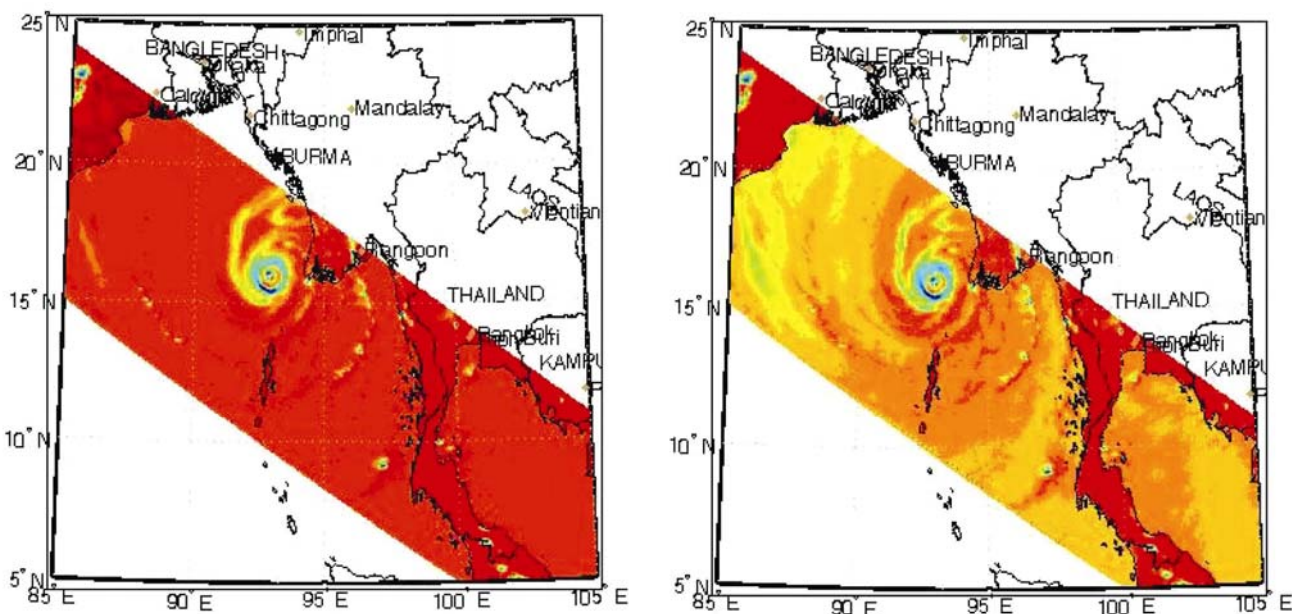


Figure 3. TMI-measured 85 GHz brightness temperature (K) for tropical cyclone MALA in vertical (left) and horizontal (right) polarization (geographical boundaries are not to scale).

TRMM PR is the first space-borne radar that measures three-dimensional reflectivity from precipitating systems¹⁴. TRMM PR scans the Earth surface at 13.8 GHz frequency with a swath of ~250 km and is sensitive to liquid precipitation subject to attenuation from cloud water and humidity. Hence, TRMM PR is ideal for matching up of liquid precipitation (from reflectivity profiles),

humidity and cloud water (from attenuation). However, it is relatively insensitive to ice particles in a rain system. Hence, in order to obtain informative a priori ice profiles, the WRF simulated ice water mixing ratios are matched up with the high-frequency channels of the TMI brightness temperatures. The flowchart of the match-up algorithm¹² for the generation of a priori is shown in Figure 4.

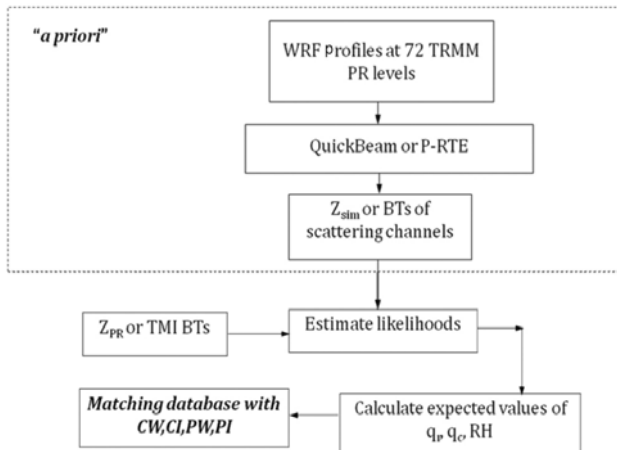


Figure 4. Profile match-up algorithm.

Bayesian-based retrieval algorithm for sample MADRAS data

A sample MADRAS observation data was provided to develop and test retrieval algorithms developed by various agencies. Nine full-orbit data scanned by the Megha-Tropiques satellite sensors on 9 December 2011 containing Level 1 and Level 2 data are available to download from an ftp website (<http://14.139.159.206/mtdata/>).

Unlike the TRMM satellite, the Megha-Tropiques does not have a radar on-board that measures the vertical reflectivity/rain profiles. Hence, it is extremely challenging to develop a rain profiling algorithm for the MADRAS imager the Megha-Tropiques with the MADRAS observation alone. The high quality a priori database of cloud liquid water, precipitating water, cloud ice and precipitating ice matched up with two of the rain-measuring instruments of TRMM, viz. the TRMM PR and the TMI in the Bayesian framework, as explained in the previous section, was found to be potentially useful in obtaining the vertical cloud and rain products from the MADRAS observations.

BTs at frequencies corresponding to the MADRAS imager of the Megha-Tropiques are simulated by the PRTE code using the WRF-TMI-TRMM PR matched-up profiles. The simulated BTs together with the WRF matched-up profiles form the a priori database for the Megha-Tropiques retrievals.

The Level 1 data products of the MADRAS imager consisting of nine BTs in two polarizations at all the frequencies, except at 23 GHz (Y) are inverted to obtain the thermodynamic and hydrometeor vertical profiles (X). The column integrated geophysical parameters retrieved by the Day 1 algorithm of the Megha-Tropiques provided in Level 2 data products were then used for comparison. The inversion was accomplished in a Bayesian framework, as discussed below.

The posterior probability density function of obtaining a state vector (X_g) given a set of observations (Y) denoted as P(X_g/Y) can be written using Bayes' theorem as follows

$$P(X_g/Y) = \frac{P(Y/X_g)P(X_g \sim X_p)}{P(Y)} \tag{6}$$

In eq. (6) X_g is the guessed rain profile. Equation (6) implies the probability that the guessed atmospheric (thermodynamic and hydrometeor) profile is the cause for the observed brightness temperatures Y is given by the product of the probability that the simulated BT is in the likelihood of measured BTs and any prior information already available about the guessed profile.

The guessed profile is generally drawn from a random sample. The simplest case of generating the guess profiles is to sample from the priori itself. For this case, the likelihood given in eq. 6 simplifies to the following expression

$$P(X_g/Y) = \exp\left(-\sum_{i=1}^9 \frac{(Y - Y_p)^2}{2\sigma^2}\right) \tag{7}$$

The value of variance inflation adjusted σ² employed in eq. (7) was 40 K. The σ² of 40 K accounts for errors in the forward model and observational errors, such as beam filling. The expected value of any parameter X given by E(X), is calculated as follows

$$E(X) = \frac{\int P(X_g/Y)X_g}{\int P(X_g/Y)} = \frac{\sum w_j X_g}{\sum w_j} \tag{8}$$

where j denotes the sample space of guess profiles. The three-dimensional hydrometeor profiles were obtained by computing the expected values given in eq. (8).

Figure 5 shows the scatter plot of wind speed retrieved using the present algorithm compared with that retrieved by Day 1 algorithm of MADRAS from Level 2 data product. From the figure, it can be seen that good agreement exists between the sample data and the present algorithm for lower wind speeds. However, for higher wind speeds, the present algorithm overestimates, when compared to the Level 2 wind speed data product. The overall correlation for the case under consideration (R) is found to be 0.86.

Figure 6 shows the scatter plot of surface rain rate retrieved using the present algorithm compared with the rain rate retrieved by Day 1 algorithm of MADRAS from Level 2 data product. Surface rain rate is one of the crucial hydrometeor parameters retrieved from the MADRAS observations that provides vital input for analysing flood and drought situations. From Figure 6, it can be seen that a reasonably good agreement exists between the sample data and the present algorithm for the entire range of rain rate. However, for lower rain rates, the present algorithm underestimates the retrieved rain rate for some cases, while overestimation of rain rate is also seen for the same range. The two trends could possibly indicate rain from

two types of rainfall – convective and stratiform. The overall correlation coefficient (R) for the case under consideration is found to be 0.77.

The column integrated liquid water (ICLW) content is compared in the last case with the geophysical parameter from the Level 2 data product. For comparison, the cloud

liquid water content profiles were integrated vertically using the formula

$$ICLW = \int_0^{18} CLW(h) dh, \tag{9}$$

where ICLW is in g/m^2 and CLW is the cloud water content retrieved for a particular layer having a thickness of dh . The integration is performed in the entire column up to a height of 18 km, which was divided with unequal spacing into 14 layers. Figure 7 shows the scatter plot between retrieved ICLW and the Level 2 data product.

Two trends emerging out with low and high cloud contents can be seen clearly from Figure 7, which is similar to what was observed with the surface rain rate. The two trends could possibly be used to delineate convective and stratiform type of clouds. The overall agreement between the two algorithms is found to be 0.68. The lower correlation coefficient is expected since it is difficult to measure cloud content from a rain event, forcing the researchers to look for an indirect algorithm to ‘measure’ the same. The not-so-high correlation coefficient also shows the lack of consistency between different algorithms to retrieve a parameter which is highly ill-posed.

Figure 8 shows the vertical structure of the retrieved hydrometeors. The structures of all the four hydrometeors are physically consistent and will serve as a crucial input in radiance/data assimilation to improve forecast skill in short-term weather prediction.

As a final inter-comparison with TRMM-TMI-derived rain estimates, the daily average rainfall for 9 December 2011 has been computed with the present algorithm and compared with the daily average rainfall reported from

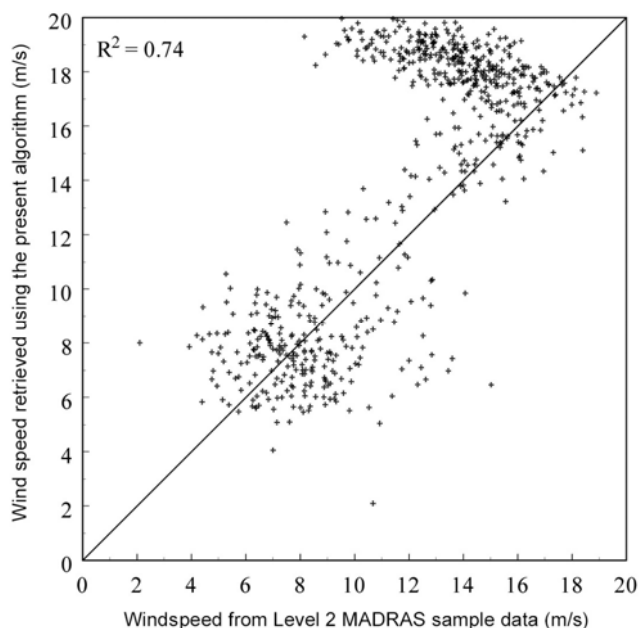


Figure 5. Scatter plot of wind speed retrieved using the present algorithm and sample data from the Level 2 data product.

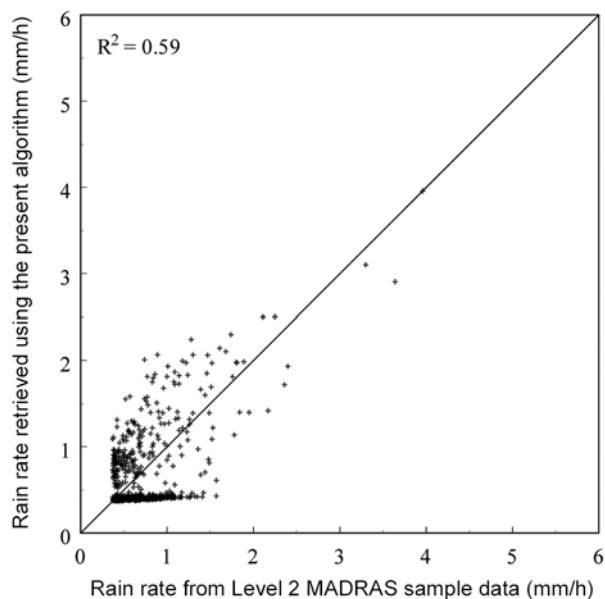


Figure 6. Scatter plot of surface rain rate retrieved using the present algorithm and sample data from the Level 2 data product.

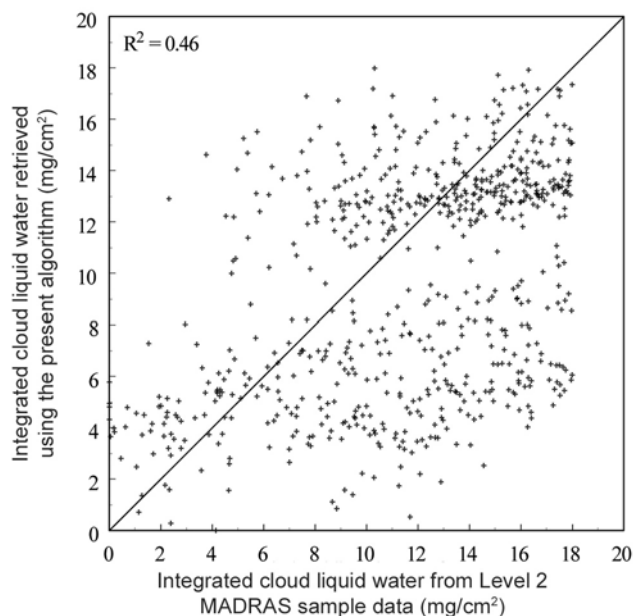


Figure 7. Scatter plot of column-integrated cloud liquid water retrieved using the present algorithm and sample data from the Level 2 data product.

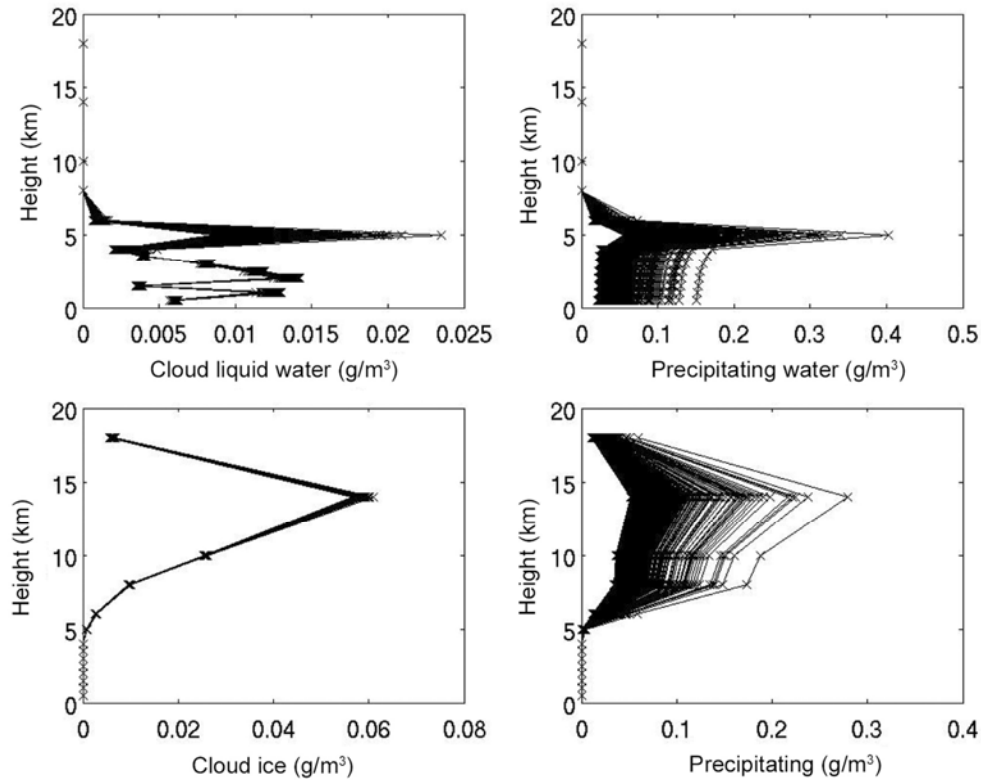


Figure 8. Vertical structure of the retrieved hydrometeors.

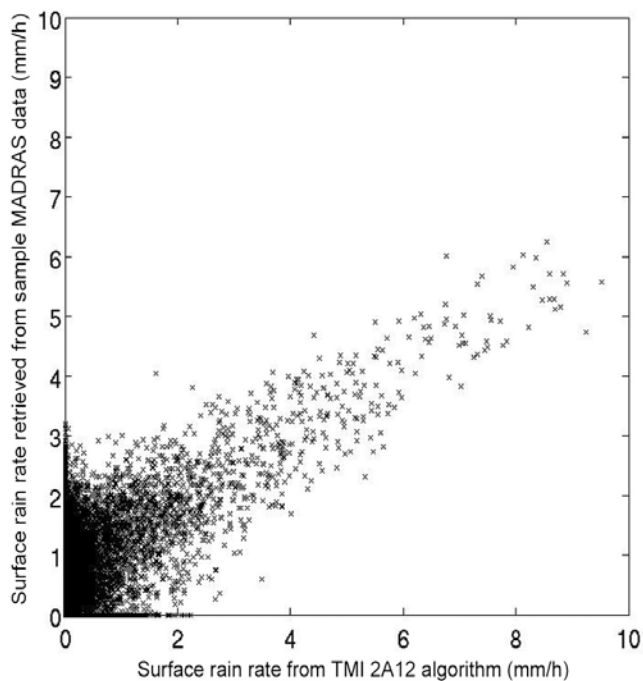


Figure 9. Comparison of daily average rain rate from TRMM and MADRAS for 9 December 2011.

TRMM-TMI. The MADRAS sample data contain BTs from nine continuous orbit scans on 9 December 2011. TMI has data from 15 orbits on the same day. Both

MADRAS and TMI data were collocated onto a common pixel of size 0.1° (~ 10 km) to obtain the common information. Daily average values of surface rain rate from both MADRAS (present algorithm) and TMI (2A12) were then calculated over pixels within 60E and 100E, 0N and 25N based on which a scatter plot was made (Figure 9). The correlation coefficient between the two estimates is 0.61. The comparison is reasonable given the approximations involved in computing the average rain from two different instruments with different orbits and channels and the approximations in converting the instantaneous rain rate into a daily average rain rate.

Further validation and fine-tuning of the algorithm and efforts to assimilate radiances from MADRAS in numerical weather prediction models are currently underway.

Conclusions

This article discussed the preliminary results from the Megha-Tropiques mission based on the research work carried out at the Indian Institute of Technology Madras. An in-house-developed polarized radiative transfer equation code was used to simulate BTs in MADRAS frequencies. Based on simulation studies, it is observed that the high-frequency channel 157 GHz shows more sensitivity towards delineating ice structures from convective events. When compared to TMI observations, the differ-

ence between 85 and 157 GHz channel BTs of up to 50 K is observed for the same rain scene.

A Bayesian-based algorithm was developed in order to retrieve vertical thermodynamic and hydrometeor profiles from nine MADRAS channels based on sample data. Initial profiles required for retrievals were obtained by running a community-based dynamics solver WRF for the rain solve. A two-way match-up of these profiles with the radar reflectivities and the radiometer BTs of the TRMM was used to develop a high-quality database that forms the backbone of the retrieval scheme. The agreement between the retrieved geophysical parameters in using high-quality a priori database and Level 2 data product of MADRAS is found to be good with R^2 of 0.74 for wind speed, 0.59 for surface rain rate retrievals and 0.46 for column-integrated cloud water content. The agreement with the TRMM daily average rain rate was found to be 0.61.

The major contribution of this work is the development of a methodology to retrieve the full vertical profile of rain and cloud in the atmosphere from the Megha-Tropiques data, which holds the key to successful radiance assimilation to improve weather prediction over the Indian subcontinent.

1. Srinivasan, J. and Narayanan, S., The Megha-Tropiques Mission. *Proc. SPIE*, 2003, doi: 10.1117/12.466703.
2. Kummerow, C., Barnes, W., Kozu, T., Shiue, J. and Simpson, J., The Tropical Rainfall Measuring Mission (TRMM) sensor package. *J. Atmos. Ocean. Technol.*, 1998, **15**, 809–817.
3. Czekala, H., Discrimination of cloud and rain liquid water path by ground based polarized microwave radiometry. *Geophys. Res. Lett.*, 1997, **25**, 1669–1672.
4. Roberti, L. and Kummerow, C., Monte Carlo calculations of polarized microwave radiation emerging from cloud structures. *J. Geophys. Res.*, 1999, **104**, 2093–2104.
5. Troitsky, A. V., Osharin, A. M., Korolev, A. V. and Strapp, J. W., Polarization of thermal microwave atmospheric radiation due to scattering by ice particles in clouds. *J. Atmos. Sci.*, 2003, **60**, 1608–1620.
6. Deiveegan, M., Balaji, C. and Venkateshan, S. P., A polarized microwave radiative transfer model for passive microwave remote sensing. *Atmos. Res.*, 2008, **88**, 277–293.
7. Marshall, J. and Palmer, W., The distribution of raindrops with size. *J. Atmos. Sci.*, 1948, **5**, 165–166.
8. Ulaby, F. T., Moore, R. K. and Fung, A. K., *Microwave Remote Sensing: Active and Passive, Vol. III – Volume Scattering and Emission Theory, Advanced Systems and Applications*, Artech House, Inc., Dedham, Massachusetts, 1986.
9. Evans, K. F. and Stephens, G. L., A new polarized atmospheric radiative transfer model. *J. Quant. Spectrosc. Radiat. Trans.*, 1991, **46**, 413–423.
10. Skamarock, W. C., Klemp, J. B., Dudhia, J., Gill, D. O., Barker, D. M., Wang, W. and Powers, J. G., A Description of the Advanced Research WRF Version 2, NCAR Technical Note, National Center for Atmospheric Research.
11. Skamarock, W. C. and Klemp, J. B., A time-split nonhydrostatic atmospheric model for weather research and forecasting applications. *J. Comput. Phys.*, 2008, **227**, 3465–3485.
12. Ooyama, K. V., A thermodynamic foundation for modeling the moist atmosphere. *J. Atmos. Sci.*, 1990, **47**, 2580–2593.
13. Ramanujam, K. S., Subramani, D. and Balaji, C., Profile correction algorithm using TRMM PR and TMI measurements in a Bayesian framework. In *Opportunities and Challenges in Monsoon Prediction in a Changing Climate*, OCHAMP-2012. Indian Institute of Tropical Meteorology, Pune, 21–25 February 2012.
14. Iguchi, T., Kozu, T., Meneghini, R., Awaka, J. and Okamoto, K., Rain – profiling algorithm for the TRMM precipitation radar. *J. Appl. Meteorol.*, 2000, **39**, 2038–2052.